Development 134, 2061-2071 (2007) doi:10.1242/dev.02853

Drosophila Nemo antagonizes BMP signaling by phosphorylation of Mad and inhibition of its nuclear accumulation

Yi Arial Zeng*,†, Maryam Rahnama*, Simon Wang, Worlanyo Sosu-Sedzorme and Esther M. Verheyen‡

Drosophila Nemo is the founding member of the Nemo-like kinase (Nlk) family of serine/threonine protein kinases that are involved in several Wnt signal transduction pathways. Here we report a novel function for Nemo in the inhibition of bone morphogenetic protein (BMP) signaling. Genetic interaction studies demonstrate that *nemo* can antagonize BMP signaling and can inhibit the expression of BMP target genes during wing development. Nemo can bind to and phosphorylate the BMP effector Mad. In cell culture, phosphorylation by Nemo blocks the nuclear accumulation of Mad by promoting export of Mad from the nucleus in a kinase-dependent manner. This is the first example of the inhibition of *Drosophila* BMP signaling by a MAPK and represents a novel mechanism of Smad inhibition through the phosphorylation of a conserved serine residue within the MH1 domain of Mad.

KEY WORDS: Nemo, Nlk, BMP, Dpp, Mad, MH1, Smad, *Drosophila*

INTRODUCTION

The *Drosophila nemo* (*nmo*) gene was originally found to be required for epithelial planar cell polarity during eye development (Choi and Benzer, 1994). Subsequent analyses have implicated *nmo* in patterning events during embryogenesis and imaginal disc development as well as in controlling apoptosis (Mirkovic et al., 2002; Verheyen et al., 2001). Nemo is the founding member of the evolutionarily conserved Nemo-like kinase (Nlk) family of proline-directed serine/threonine (S/T) kinases closely related to mitogen-activated protein kinases (MAPK) (Choi and Benzer, 1994).

Biochemical and genetic studies implicate Nlk in several pathways (reviewed by Behrens, 2000; Martinez Arias et al., 1999). The best-characterized role for Nlk is in Wnt/Wg signaling in numerous species (Golan et al., 2004; Ishitani et al., 2003a; Ishitani et al., 1999; Kanei-Ishii et al., 2004; Meneghini et al., 1999; Rocheleau et al., 1999; Shin et al., 1999; Smit et al., 2004; Thorpe and Moon, 2004; Zeng and Verheyen, 2004). Nlk phosphorylates Tcf/Lef transcription factors and inhibits their activity. Depending on the cellular context, Nlk either inhibits Wnt-dependent gene expression (Ishitani et al., 2003b; Ishitani et al., 1999; Zeng and Verheyen, 2004) or promotes it (Meneghini et al., 1999; Rocheleau et al., 1999; Thorpe and Moon, 2004). There is increasing evidence that Nlk regulates additional HMG-domain-containing proteins, such as *Xenopus* Sox11 and HMG2L1 (Hyodo-Miura et al., 2002; Yamada et al., 2003), as well as other transcriptional regulators such as CBP/p300, Stat3 and Myb (Kanei-Ishii et al., 2004; Ohkawara et al., 2004; Yasuda et al., 2004).

Nlk can be activated by the MAPK kinase kinase Tak1 (TGF-β activated kinase 1) in mammals (also known as Map3k7 – Mouse Genome Informatics) and in *C. elegans* (also known as MOM-4 – Wormbase) in certain contexts (Ishitani et al., 1999; Meneghini et al., 1999). However, in this study we describe an inhibitory relationship between Nemo and *Drosophila* TGF-β signaling. TGF-β signaling is initiated when a secreted ligand of the TGF-β, bone morphogenic protein (BMP) or Activin family binds to a type II S/T kinase receptor (reviewed by Attisano and Wrana, 2002; von Bubnoff and Cho, 2001). This receptor then recruits and phosphorylates a type I S/T kinase receptor, which in turn phosphorylates a member of the R-Smad family of proteins on an SSxS motif at its C-terminus. The phosphorylated R-Smad is released from the receptor and binds the Co-Smad. In the nucleus, the Smad complex forms complexes with transcription factors on the promoters of target genes. Nuclear signaling is abrogated when the R-Smad is dephosphorylated at its C-terminus (Chen et al., 2006; Duan et al., 2006; Knockaert et al., 2006).

During *Drosophila* wing patterning, BMP signaling is carried out by two BMPs, Decapentaplegic (Dpp) and Glass bottom boat (Gbb) (Padgett et al., 1987; Wharton et al., 1991). Dpp acts as a morphogen during the patterning of multiple tissues during embryonic and imaginal disc development (reviewed by Raftery and Sutherland, 1999). Dpp activates the Punt receptor, which in turn phosphorylates Thickveins (Tkv), leading to the activation of the Smads. The Smad1 ortholog, Mothers against dpp (Mad), is phosphorylated by activated Tkv and together with the Co-Smad Medea (Med) accumulates in the nucleus and regulates transcription of target genes (reviewed by Moustakas et al., 2001; Shi and Massague, 2003; ten Dijke and Hill, 2004). In the wing imaginal disc, BMP signaling regulates the expression of several genes, including *optomoter blind* (*omb*; also known as *bifid* – Flybase), *spalt major* (*salm*) and *vestigial* quadrant (vg^{Q}) enhancer (Burke and Basler, 1996; Grimm and Pflugfelder, 1996; Kim et al., 1997; Lecuit et al., 1996; Lecuit and Cohen, 1998; Nellen et al., 1996). The inhibitory Smad homolog *Daughters against dpp* (*Dad*) is also a BMP target gene that acts in a negative-feedback loop to inhibit BMP signaling (Tsuneizumi et al., 1997).

Dpp plays several distinct roles during larval and pupal wing development (Segal and Gelbart, 1985; Spencer et al., 1982). During larval disc development, Dpp is expressed along the anterior/posterior (A/P) boundary of the disc in response to

Department of Molecular Biology and Biochemistry, Simon Fraser University, Burnaby, British Columbia, V5A 1S6, Canada.

*These authors contributed equally to this work
†Present address: Department of Developmental Biology, Stanford University, Stanford, CA 94305-5323, USA
‡Author for correspondence (e-mail: everheye@sfu.ca)

Accepted 19 March 2007

Hedgehog signaling (Tanimoto et al., 2000). Localized phosphorylation and activation of Mad (pMad) results in a Mad activity gradient that drives characteristic patterns of reporter gene expression across the wing disc, providing positional information to guide wing vein organization. In addition to a patterning function, BMP signaling is required for proliferation of the disc, as clones of cells lacking *tkv* or *Mad* are smaller than sister clones and are eliminated from the wing disc, whereas ectopic BMP signaling results in outgrowths (Martin-Castellanos and Edgar, 2002; Rogulja and Irvine, 2005). It is speculated that the slope and extent of the pMad gradient is important for both the proliferative and patterning functions of Dpp, but the temporal and spatial characteristics for each are distinct (Rogulja and Irvine, 2005).

In this study we describe a detailed analysis of a novel interaction between *nmo* and BMP signaling mediated by Mad. Genetic studies in the wing suggest a role for *nmo* as an antagonist of BMP signaling. These genetic interactions are supported by the finding that elevated Nemo levels can attenuate BMP target gene expression, whereas loss of *nmo* results in elevated target gene expression. Biochemical and cell culture studies show that Nemo can bind to and phosphorylate Mad and promote its nuclear export. Nemo phosphorylates the MH1 domain of Mad at Ser25 and mutation of this site to alanine causes ligand-independent nuclear localization, whereas substitution with the phosphomimetic aspartic acid results in cytoplasmic localization of Mad. This is the first example of the inhibition of *Drosophila* BMP signaling by a MAPK and represents a novel mechanism of Smad inhibition by a Nemo-like kinase family member.

MATERIALS AND METHODS

Fly strains

The following fly strains were used: nmo^{DB24} (Zeng and Verheyen, 2004), nmo^{adk1} and *UAS-*$nmo^{C5\text{-}1e}$ (Verheyen et al., 2001), *UAS-*nmo^{b27}, nmo^{P} also referred to as *nmo-lacZ* (Choi and Benzer, 1994; Zeng and Verheyen, 2004), *AyGal4.25-UAS-GFP.S65T* (Ito et al., 1997; Zecca et al., 1996), *Ubi-GFP FRT* 79D, *ap-Gal4* (expressed in the dorsal wing disc compartment), *dpp-Gal4* (expressed along the A/P boundary), *ptc-Gal4* (expressed along the A/P boundary), *vg-Gal4* (expressed along the D/V boundary), *prd-Gal4* (expressed in alternating stripes in the embryo), *69B-Gal4* (expressed ubiquitously in the wing pouch), *omb-Gal4* (expressed in a wide domain along the A/P axis in the wing pouch), dpp^{d5}, dpp^{hr56}, dpp^{hr4}, *UAS-Mad*, *UAS-MadS25A*, *UAS-*tkv^{QD} (Nellen et al., 1996), *UAS-*tkv^{wt}, *UAS-sog* (Yu et al., 2000), *P{lacW}Dad*^{j1E4} (Tsuneizumi et al., 1997), vg^{Q}*-lacZ*, *salm-lacZ*, rl^{Sem}*/CyO*, *UAS-*$Sem^{3\text{-}1}$ (Rintelen et al., 2003) and *UAS-GFP*.

Clonal analysis

nmo^{DB24} somatic clones were induced using the FLP/FRT method (Xu and Rubin, 1993). To induce *nmo* loss-of-function clones, embryos from the appropriate crosses were collected for 24 hours and the hatched larvae were heat shocked at 38°C for 90 minutes at 48 hours of development. More than 30 clones were examined in each experiment.

Immunostaining and wing handling

Dissection of imaginal discs, X-Gal staining and antibody staining were performed following standard protocols. The antibodies used were: rabbit anti-pMad (1:1000) (Persson et al., 1998), anti-Delta 9B ascites (1:5000; DSHB), mouse anti-β-galactosidase (1:500; Promega) and rabbit anti-β-galactosidase (1:2000; Cappel). Secondary antibodies used were: donkey anti-mouse FITC, donkey anti-rabbit CY3, donkey anti-rabbit FITC and biotinylated goat anti-rabbit (all from Jackson ImmunoResearch), donkey anti-mouse Alexa Fluor 594 (Molecular Probes). All secondary antibodies were used at a 1:200 dilution.

Adult wings were dissected and rinsed in 100% ethanol followed by mounting in Aquatex (EM Science).

Nemo expression vectors

Full-length *nmo* coding sequences were cloned into the pXJ-Flag expression vector. The kinase-dead Nemo construct encodes a substitution of a lysine residue at position 69 for a methionine (K69M). This was modeled on the kinase-dead form of Nlk described by Brott et al. (Brott et al., 1998). Mutagenesis was performed using the QuickChange Site-Directed Mutagenesis Kit according to the manufacturer's instructions (Stratagene).

Co-immunoprecipitations

HEK293 cells were cultured in Dulbecco's modified Eagle's medium (DMEM; Gibco) supplemented with 10% fetal bovine serum (Gibco). Cells at 70-80% confluency were subjected to transient transfection with 8 μg total DNA using Polyfect transfection reagent (Qiagen) following the manufacturer's instruction. Cells were lysed 24-48 hours after transfection in lysis buffer [10% glycerol, 1% Triton X-100, 50 mM Tris pH 7.5, 5 mM EDTA, 150 mM NaCl, 4% protease inhibitors (Roche), 100 mM β-glycerol phosphate, 1 mM sodium vanadate, 5 mM NaF]. Mouse anti-Flag (Sigma) or mouse anti-T7 (Novagen) coupled to protein G-sepharose beads (Sigma) were used for immunoprecipitation for 1 hour at 4°C. The immunocomplexes were washed three times with lysis buffer and boiled in Laemmli buffer, then subjected to SDS-PAGE and western analysis according to standard protocols. Primary antibodies used were mouse anti-Flag (1:1000) or mouse anti-T7 (1:5000), and the secondary antibody was goat anti-mouse HRP light chain-specific (1:5000; Jackson ImmunoResearch). The western blot was visualized using the Enhanced Chemiluminescence (ECL) Western Blotting System (Amersham).

Kinase assays

Cell lysates were precleared with protein G-sepharose beads and incubated with appropriate antibodies. Antibody-protein complexes were precipitated with protein G-sepharose beads, then washed three times with lysis buffer and once with kinase assay buffer (25 mM HEPES pH 7.2, 25 mM $MgCl_2$, 50 mM β-glycerol phosphate, 2 mM dithiothreitol, 0.5 mM sodium vanadate, 0.1 mM ribo-ATP). Kinase reactions were initiated by the addition of kinase assay buffer containing 10 μCi of [γ-^{32}P]ATP at room temperature and stopped after 20 minutes by the addition of Laemmli buffer. Samples were boiled and subjected to SDS-PAGE and transferred to nitrocellulose membrane (Perkin Elmer Life Sciences) according to standard protocols and visualized by autoradiography.

Immunostaining of cultured cells and nuclear export assays

COS-7 and HeLa cells were grown on glass coverslips in 6-well plates 24 hours prior to transfection. Cells at 50-70% confluency were transiently transfected with various combinations of vectors: pCMV-T7-mad; pCMV-T7-mad and pCDNA-HA-tkv^{QD} (Inoue et al., 1998); pCMV-T7-mad, pCDNA-HA-tkv^{QD} and pXJ-Flag-nmo; pCMV-T7-mad, pCDNA-HA-tkv^{QD} and pXJ-Flag-nmo^{K69M}; pCMV-T7-mad-S25A; pCMV-T7-mad-S25D. Sixteen hours post-transfection, the cells were fixed in 4% paraformaldehyde for 15 minutes, followed by permeabilization with 0.25% Triton X-100. Following two washes in PBS, immunostaining was performed using mouse anti-T7 antibody (1:2000; Novagen) and rabbit anti-HA (1:1000; Sigma). Secondary staining was performed using donkey anti-mouse FITC and goat anti-rabbit CY3 (1:200). Coverslips were mounted cell-side down with Prolong Gold Antifade Reagent with DAPI (Molecular Probes). For Crm1-dependent nuclear export assays, leptomycin B (Sigma) was added to a final concentration of 5.53 ng/ml for 2 hours prior to fixation.

Site-directed mutagenesis of Mad and generation of the Mad MH1 deletion construct

Mutagenesis was performed on the pCMV-T7-mad plasmid, using the QuickChange Site-Directed Mutagenesis Kit according to the manufacturer's instructions (Stratagene). Forward and reverse PCR primers were designed to harbor several nucleotide changes, with the rest of the sequence corresponding to the template. Serines 25, 146, 202, 212 and 226 were respectively substituted with alanines as indicated in Fig. 6. In addition, S25 was replaced with aspartic acid (S25D) to introduce a phosphomimetic residue.

The Mad-ΔMH1 construct was made by excision of an *Eco*RI fragment from the 5′ coding region of the pCMV-T7-mad plasmid. pCMV-T7-mad contains two *Eco*RI sites: one is located in the 5′ multiple cloning site, the

other is at the boundary of the MH1 domain and the linker domain. Mad-ΔMH1 was obtained by *Eco*RI digestion, gel purification of the vector plus 3′ sequences and religation resulting in an in-frame fusion of T7 with the remainder of the Mad coding region, thereby deleting the MH1 domain.

Untagged and T7-tagged MadS25A were cloned into pUAST and transgenic fly strains were generated by BestGene. The *prd-Gal4* driver was used to express this transgene in alternating embryonic segments and *en-Gal4*, *ap-Gal4* and *vg-Gal4* were used to test for phenotypic effects in the wing.

RESULTS

nmo wing phenotypes suggest antagonism of BMP signaling

Modulation of *nmo* expression affects the patterning and growth of multiple tissues (Choi and Benzer, 1994; Mirkovic et al., 2002; Verheyen et al., 2001). Notably, the wing phenotypes are indicative of altered BMP signaling. The adult wing blade consists of two epithelial sheets of intervein cells intersected at regular intervals by an invariant pattern of longitudinal veins (numbered L2-L5), the anterior crossvein (ACV) and posterior crossvein (PCV) (Fig. 1A) (Bier, 2000). Mutations that target the early role of Dpp result in vein loss, vein fusions and narrowing of wing tissue (Fig. 1B,C) (Cook et al., 2004; Haerry et al., 1998; Segal and Gelbart, 1985; Spencer et al., 1982). Later, during pupal wing development, *dpp* expression in vein primordia functions to maintain and refine the veins (de Celis, 1997; Yu et al., 1996).

Ectopic expression of Nemo using the Gal4-UAS system causes a number of different wing phenotypes (Brand and Perrimon, 1993; Mirkovic et al., 2002; Verheyen et al., 2001; Zeng and Verheyen, 2004). Expression of *nmo* with *omb-Gal4* resulted in a narrowing of the regions between longitudinal veins, notably L2 and L3 (Fig. 1D), a phenotype seen with certain *dpp* alleles (Brummel et al., 1994; Segal and Gelbart, 1985). Expression of two copies of *UAS-nmo* with *omb-Gal4* (*omb>2x nmo*) resulted in loss of wing tissue, narrowing of the interval between veins, loss of the PCV and loss of some longitudinal veins (Fig. 1E,F). This phenotype is reminiscent of BMP inhibition caused by *brinker* (Cook et al., 2004), and phenocopies that seen with expression of dominant-negative versions of the Dpp receptors *tkv* and *punt* (Haerry et al., 1998) and in certain *dpp* mutants (Bangi and Wharton, 2006). *69B-Gal4>nmo* results in varied loss of the PCV and a narrower wing blade (Fig. 1J) (Verheyen et al., 2001). This phenotype resembles loss-of-function mutations in the *gbb*, *Medea* and *crossveinless* genes (Conley et al., 2000; Hudson et al., 1998; Khalsa et al., 1998; Segal and Gelbart, 1985). Similarly, ectopic expression of the BMP antagonist *sog* also leads to loss of PCV tissue (Fig. 1I) (Yu et al., 1996).

By contrast, *nmo* loss-of-function alleles displayed a broader wing blade and ectopic veins emanating from the PCV, posterior to L5 and between L2 and L3 (Fig. 1H). The distance between the longitudinal veins was also expanded (Fig. 2H; see below). The *nmo* phenotype is similar to those found in flies ectopically expressing Dpp, Mad or Gbb (Haerry et al., 1998; Yu et al., 2000; Yu et al., 1996). Using *vestigial-Gal4* (*vg-Gal4*) to express *UAS-Mad* along the dorsal/ventral (D/V) boundary also resulted in a broader wing and ectopic veins along L2 and L5 and emanating from the PCV (Fig. 1G) (see also Tsuneizumi et al., 1997). This affect on wing shape, size and vein position in loss-of-function and ectopic *nmo* flies suggests that Nemo might negatively influence BMP signaling.

Modulation of Nemo affects wing disc proliferation

To quantitate the effect of Nemo on the width of the wing blade and the spacing of veins as processes directly regulated by BMP signaling, we measured wing blades of different genotypes. Superimposition of wild-type and *nmo* wings (Fig. 2A-C) showed that the positions of L2 and L5 are shifted from the central A/P boundary towards the margins in *nmo* wings. The abnormal vein positions in both genotypes were statistically significant (Fig. 2H) and highly reproducible; namely, *nmo* mutant wings showed an almost identical pattern of vein spacing. Conversely, ectopic Nemo in *omb>nmo* caused a shift of L2 and L5 towards the A/P boundary (Fig. 2D-F).

To address whether the abnormal wing size in *nmo* mutants is a result of changes in cell proliferation, we determined cell density within a given region in the wing blade (Fig. 2I-L, Table 1) and also measured overall wing area. Each wing blade cell possesses a single hair (trichome) and counting trichomes thus reflects cell number. *nmo* wings possessed more cells per given area, and this difference was statistically significant (Table 1, $P<0.01$). This suggests that *nmo* mutant cells are slightly smaller than wild type cells. Area measurements determined that *nmo* wings were consistently larger than wild type wings (Table 1, $P<0.0001$). This indicates that there is more proliferation in a *nmo* wing. Since BMP signaling is required for proliferation, it follows that a putative antagonist of the pathway would normally act to inhibit growth, and its mutation would result in increased growth.

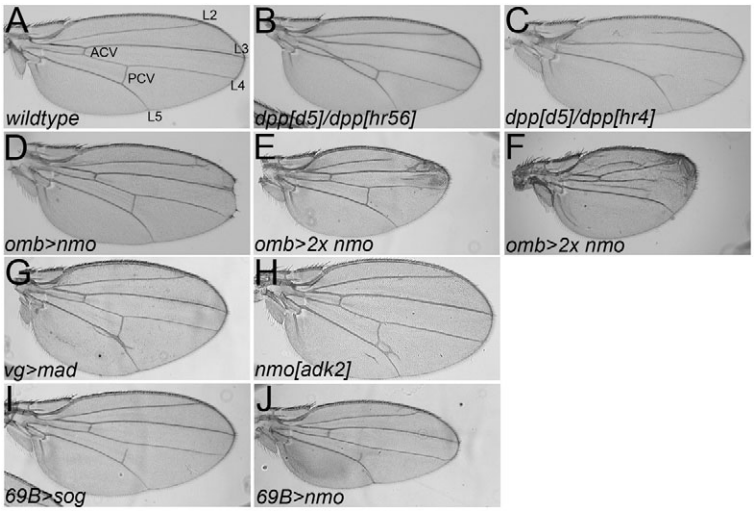

Fig. 1. Opposing effects of *nmo* and the Dpp pathway on *Drosophila* wing growth and patterning. (**A**) A wild-type adult wing. (**B**,**C**) Wings from transheterozygous combinations of *dpp* loss-of-function alleles (B, dpp^{d5}/dpp^{hr56}; C, dpp^{d5}/dpp^{hr4}) show reductions in vein spacing and loss of veins. (**D-F**) Ectopic Nemo decreases spacing of veins in a dose-sensitive manner. (D) *omb-Gal4/+; UAS-nemo/+*. (E,F) *omb-Gal4/+; UAS-nmo/+; UAS-nmo/+*. (**G**) *UAS-Mad/+; vg-Gal4/+*. (**H**) A nmo^{adk2}/nmo^{adk2} loss-of-function wing. (**I**) Ectopic expression of the BMP antagonist Sog (*UAS-sog/+; 69B-Gal4/+*). (**J**) *UAS-nmo/+; 69B-Gal4/+* phenocopies reduced BMP signaling.

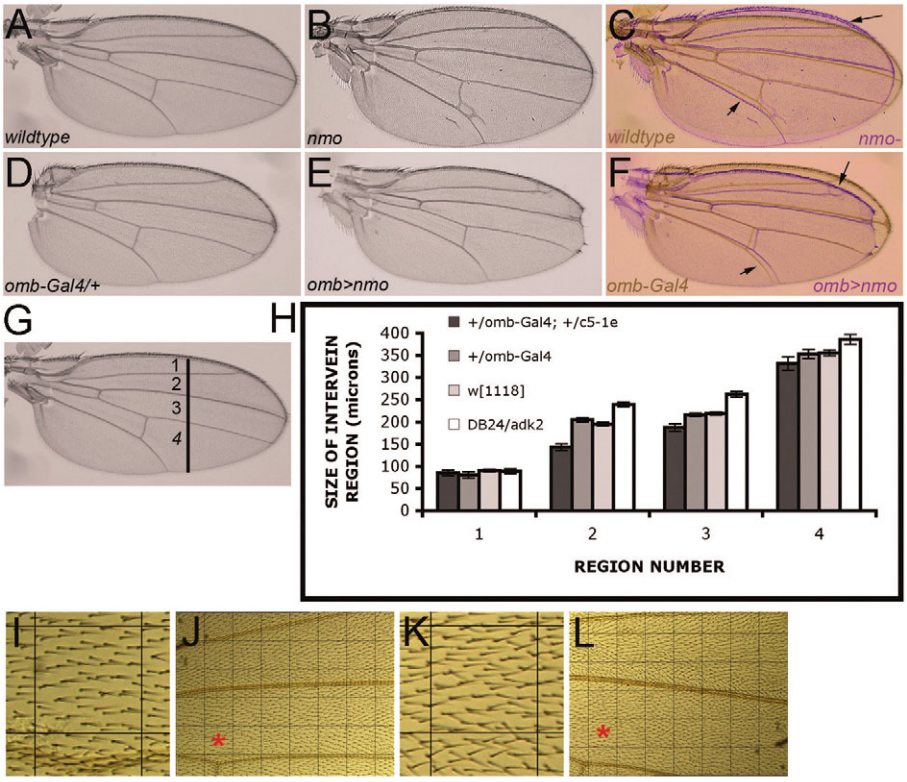

Fig. 2. Modulation of Nemo affects the spacing of veins and wing cell density. (**A-C**) Comparison of intervein distances between wild-type (A) and nmo^{adk2}/nmo^{adk2} (B) *Drosophila* wings. (C) Superimposition of the two wings, showing that *nmo* L2 and L5 veins (arrows) are spaced further apart than in the wild type. (**D-F**) Comparison of intervein distances between an *omb-Gal4/+* control (D) and *omb-Gal4/+; UAS-nmo/+* (E). (F) Superimposition of the two wings, showing that *omb>nmo* L2 and L5 veins (arrows) are closer together than in the *omb-Gal4* control. (**G**) A wild-type wing with the numbering scheme depicted for the measured intervals, 1-4. (**H**) Measurement of intervein regions in the wild type, *omb-Gal4/+*, *omb>nmo* and nmo^{adk2}. (**I-L**) Cell density within a given region in the wing blade of the wild type (I,J) and nmo^{adk2}/nmo^{adk2} (K,L) was calculated by counting trichome density in the indicated squares (I,K; the location of the counted regions is indicated with an asterisk in J,L). The results are shown in Table 1.

nmo is an antagonist of BMP signaling

To test the hypothesis that Nemo inhibits BMP signaling we carried out genetic interaction studies. Several *Gal4*-driver strains were used to activate BMP signaling, and the ability of *nmo* to modulate the induced phenotypes was then examined. In all cases, expression of *UAS-nmo* caused a dramatic reduction in the severity of phenotypes resulting from activation of BMP signaling. Specifically, constitutively active Tkv driven by *dpp-Gal4* ($UAS\text{-}tkv^{QD}$) (Nellen et al., 1996) resulted in a 20.8% penetrant bifurcated wing blade phenotype (n=53), which was completely suppressed by co-expression of *UAS-nmo* (Fig. 3A-C; n=49). Although the bifurcation was suppressed, ectopic *nmo* was unable to fully restore the wing to wild-type morphology. Use of *patched* (*ptc-Gal4*) to drive expression of wild-type *UAS-tkv* caused a vein defect along the A/P boundary (Fig. 3D) that was suppressed by *UAS-nmo* (Fig. 3F). Marquez et al. (Marquez et al., 2001) also observed ectopic vein phenotypes upon ectopic expression of Mad. *vg>Mad* caused a broader wing shape and an abnormal wing vein phenotype (Fig. 1G, Fig. 3G). Whereas *vg>nmo* caused no discernable phenotype (Fig. 3H), co-expression of *UAS-nmo* and *UAS-Mad* led to dose-sensitive suppression of the phenotype induced by *UAS-Mad* (Fig. 3I), as two copies of Nemo almost completely suppressed the *vg>Mad* phenotype (Fig. 5D).

In addition to suppression of activated BMP phenotypes, flies heterozygous for the nmo^{P} hypomorphic mutation showed an enhancement in the penetrance of the $dpp>tkv^{QD}$ bifurcated wing phenotype from 20.8% to 86.3%. This finding demonstrates that reduction of *nmo* can lead to even higher levels of BMP signaling.

The observation of a synergistic interaction between *nmo* and *Dad* provided further support for the proposal that Nemo antagonizes BMP signaling. Dad is an antagonist that is also a transcriptional target of the pathway (Tsuneizumi et al., 1997). A P-element enhancer trap insertion into the *Dad* gene caused no discernible wing phenotype in homozygous flies (Fig. 3J), yet in the $Dad^{j1E4}; nmo^{adk1}$ double-mutant fly we observed ectopic vein phenotypes much more severe than nmo^{adk1} normally displayed (Fig. 3, compare L with K). This suggests that both genes contribute to the inhibition of the pathway and that this *Dad* allele might have partially reduced function, but not below the threshold needed to see a defect on its own.

Nemo can modulate BMP-dependent gene expression

To further characterize the inhibitory effect of *nmo*, the expression of BMP-target genes was monitored in third instar larval wing discs bearing either *nmo* mutant clones or ectopic expression of *nmo*. The *vestigial* quadrant (vg^{Q}) enhancer is expressed in domains flanking the D/V and A/P boundaries (Fig. 4A). Mad has been shown to bind directly to the Dpp-responsive element within the vg^{Q} enhancer (Kim et al., 1997); thus, this gene serves well as a readout of Mad-mediated gene expression. *UAS-nmo* driven by the dorsally

Table 1. Altered cell density and area of wing blades in the *nmo* mutant

Density of wing blade cells within a defined area*				
	Cell no.	s.d.	n	
Wild type	69.33	2.81	12	
nmo^{adk2}/nmo^{db24}	73.25	3.67	12	P<0.01
Area of wing blade†				
	Relative area	s.d.	n	
Wild type	1.404	0.083	25	
nmo^{adk2}/nmo^{db24}	1.677	0.052	34	P<0.0001

*Each wing blade produces a single hair, which was counted within a box of fixed size and position (as shown in Fig. 2) to give overall cell density.
†Area was measured using ImageJ software by outlining the circumference and measuring relative area.

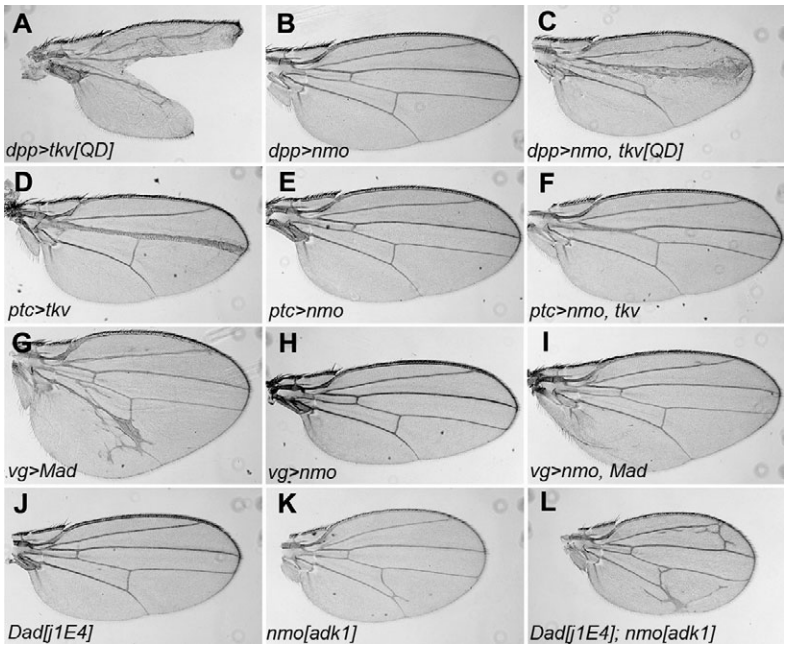

Fig. 3. *nmo* antagonizes BMP signaling during *Drosophila* wing development. (**A**) *dpp-Gal4>UAS-tkv^{QD}* results in a bifurcated wing blade. (**B**) *dpp-Gal4>UAS-nmo* has no visible wing defect. (**C**) Ectopic *nmo* is able to suppress the bifurcated phenotype in *UAS-nmo/+; dppGal4/UAS-tkv^{QD}* wings. (**D**) *ptc-Gal4>UAS-tkv* causes loss of wing tissue and fusion of L3 and L4 veins. (**E**) *ptc-Gal4>UAS-nmo* shows no obvious phenotype. (**F**) *ptc-Gal4/UAS-nmo; UAS-tkv/+* shows suppression of the ectopic *tkv* phenotype. (**G**) *vg-Gal4>UAS-Mad* showing both a widened wing blade and ectopic veins. (**H**) *vg-Gal4>UAS-nmo* shows no obvious phenotype. (**I**) *UAS-Mad/+; vg-Gal4/UAS-nmo* rescues the broad wing blade and ectopic wing veins phenotype caused by ectopic *Mad*. (**J**) The weak *Dad* mutant *Dad^{j1E4}* has no discernible wing phenotype. (**K**) *nmo^{adk1}* showing a mild ectopic vein phenotype. (**L**) *Dad^{j1E4}; nmo^{adk1}* double-mutants have more severe ectopic vein phenotypes than *nmo^{adk1}* alone.

expressed *apterous-Gal4* severely reduced *vg^{Q}-lacZ* staining in the dorsal wing pouch (Fig. 4B). To further characterize this effect, *vg^{Q}* expression was monitored in wing discs containing *nmo* loss-of-function somatic clones (Fig. 4C-E). *nmo^{DB24}* clones in the central region of the wing where Dpp signaling is most active (and *nmo* is normally enriched, see Fig. 4I) showed elevated *vg^{Q}* expression (Fig. 4E, arrow), whereas clones outside of this region showed no change in reporter gene expression (Fig. 4E, arrowhead).

The narrowed wing seen in *omb>2x nmo* (Fig. 1F) flies suggests an inhibition of Mad signaling, which sets up the width of wing vein intervals. Staining for the target gene *salm* confirmed that modulation of *nmo* can affect the width of the BMP response gradient. *salm* is expressed in the central portion of the wing pouch and the breadth of the strip indicates the degree of BMP signaling (Fig. 4) (Barrio and de Celis, 2004; Lecuit and Cohen, 1998; Sturtevant et al., 1997). Measurements of the width of *salm* expression at the D/V boundary (Fig. 4, white lines) were normalized against wild type (taken as 100%). In *nmo* mutants, the width of the *salm* domain was consistently wider than in the wild type (113.92%, *n*=20, Fig. 4G), whereas in *omb>2x nmo* the width was dramatically reduced to just 56.62% (*n*=20, Fig. 4H).

nmo has a dynamic expression pattern in wing discs (Verheyen et al., 2001; Zeng and Verheyen, 2004). In addition to expression along the D/V boundary, in late third instar wing discs *nmo* is enriched in two stripes flanking the A/P boundary of the wing and is expressed ubiquitously throughout the disc at lower levels (Fig. 4I). This expression overlaps with the peaks of pMad staining and corresponds to the site of the future longitudinal veins L3 and L4 (Fig. 4I-K) (Tanimoto et al., 2000). During pupal wing development, *nmo* is expressed in intervein regions and is enriched in the cells flanking the presumptive veins (Verheyen et al., 2001). This pattern of expression together with phenotypic observations suggest a role for *nmo* during BMP function in vein patterning and refinement (Conley et al., 2000).

To determine if *nmo* can affect levels of pMad, we examined pMad antibody staining in *nmo* mutant clones. In *nmo^{DB24}* mutant clones (Fig. 4L, marked by the absence of GFP fluorescence) there was no detectable change in the levels of pMad (Fig. 4N and merged image in Fig. 4M). In *omb>1x nmo* discs where the width of the *salm* expression domain was altered (data not shown), we observed a slight narrowing of the interval between pMad stripes (Fig. 4Q), whereas in homozygous *nmo* mutant discs the domain was subtly wider (Fig. 4P). Although the mechanism responsible for this observation is not yet known, it is possible that the early role of Nemo in regulating proliferation affects cell numbers in the disc and wing (Fig. 2, Table 1).

Inhibition of Mad is specific to Nemo and not a general feature of MAPK in *Drosophila* wings

There is a precedent for inhibition of Smad signaling by MAPK proteins from a number of studies using mammalian cell culture (Aubin et al., 2004; Grimm and Gurdon, 2002; Kretzschmar et al., 1997; Kretzschmar et al., 1999; Pera et al., 2003). We sought to examine whether *Drosophila* Erk MAPK, encoded by the *rolled* (*rl*) locus, could play a similar role. In flies, both Epidermal growth factor receptor (Egfr) and BMP signaling are required for vein specification (Bier, 2000). Hyperactivity of Erk, as found in the *rl^{Sem}* allele, results in ectopic veins (Fig. 5C) (Brunner et al., 1994), similar to those seen upon loss of *nmo* (Fig. 1H). Whereas co-expression of Nmo and Mad suppressed the ectopic veins induced by *Mad* (Fig. 3I, Fig. 5D), the combination of ectopic *Mad* and *rl^{Sem}* (either through ectopic expression of a *UAS-rl^{Sem}* transgene or introduction of the *rl^{Sem}* hypermorphic mutation) resulted in an extreme synergistic vein promotion and excess proliferation (Fig. 5E,F). We conclude that in this context, Erk MAPK does not inhibit Mad signaling.

Nemo binds to and phosphorylates Mad

Since Nemo can genetically inhibit BMP signaling, we sought to address the underlying biochemical mechanism. Nlk can target a number of transcriptional regulators and affect their function both positively and negatively. Since Nemo can antagonize Mad-dependent target gene expression in vivo, co-immunoprecipitation studies were carried out. HEK293 cells were transfected with T7-tagged Mad and Flag-tagged Nemo and immunoprecipitations revealed binding of Mad and Nemo (Fig. 6A).

Next we addressed whether Nemo could phosphorylate Mad. In vitro kinase assays were performed on cell lysates and Nemo was found to phosphorylate Mad, as well as to autophosphorylate (Fig. 6B). This was dependent on the kinase activity of Nemo as a dominant-negative Nemo (K69M) construct, in which the lysine residue in the ATP-binding domain was changed to methionine, did not show phosphorylation of Mad, nor did it show Nemo autophosphorylation (Fig. 6B).

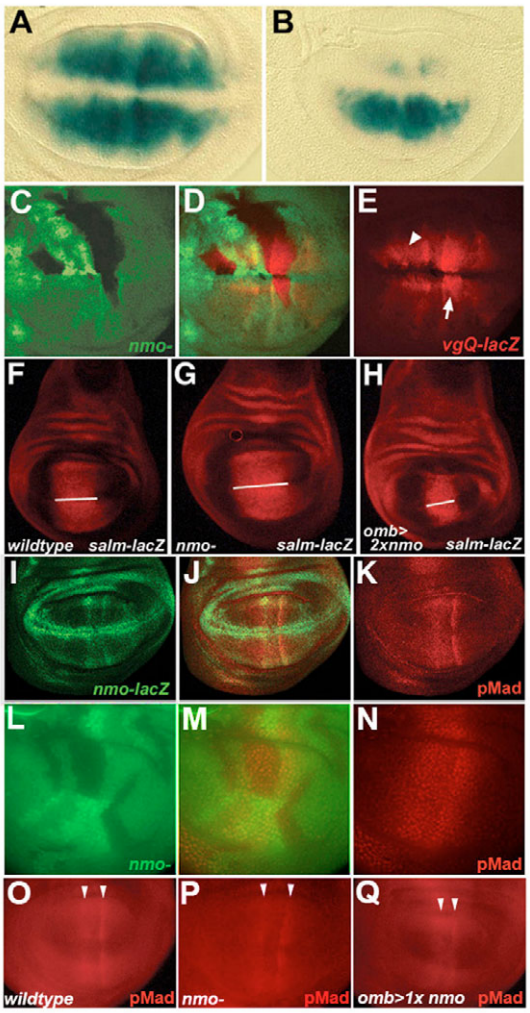

Fig. 4. *nmo* modulates Mad-dependent target gene expression and the pMad gradient. (**A**) vg^{Q}-*lacZ* expression in the wild-type *Drosophila* third instar wing imaginal disc. (**B**) vg^{Q} expression is abolished in the dorsal wing pouch when *UAS-nmo* is expressed using the dorsal-specific driver *ap-Gal4*. (**C**,**D**) nmo^{DB24} somatic clones (marked by the absence of GFP, green). (**E**) Expression of vg^{Q}-*lacZ* is increased in the clone abutting the A/P boundary (arrow) but shows no detectable change in the clone further away from the levels of highest Dpp signaling, in which *nmo* expression is normally low (arrowhead). (**F-H**) Salm expression in wild-type, nmo^{DB24}/nmo^{adk2} and *omb>2x nmo* third instar wing discs. The width of Salm expression along the D/V boundary is indicated by a white line. (**I-K**) nmo^{lacZ} expression in late third instar stage wing discs (green) co-localizes in the L3 and L4 vein primordia flanking the A/P boundary with highest levels of pMad staining (red in J,K). (**L-N**) nmo^{DB24} somatic clones (marked by the absence of GFP, green). (M,N) pMad staining is unchanged in *nmo* clones. (**O-Q**) pMad staining in wild-type (O), nmo^{DB24}/nmo^{adk2} (P) and *omb>1x nmo* (Q) discs. Arrowheads indicate the position of peaks of pMad staining.

Nemo targets serine 25 in the MH1 domain of Mad

The Mad protein consists of a highly conserved N-terminal Mad homology domain 1 (MH1), a non-conserved linker region and the conserved C-terminal MH2 domain (Fig. 6C) (reviewed by Kretzschmar and Massagué, 1998). Since Nemo is a proline-directed S/T kinase, we sought to identify Nemo target residues in Mad. We identified all S/T residues followed directly by prolines (S/TP). Based on the precedent seen with Erk-mediated inhibition of Smads, we first targeted residues within the linker region of Mad. Site-directed mutagenesis was employed to alter serine 212 (S212) to alanine in the single consensus Erk phosphorylation site (PNSP) in the linker domain. In addition, two putative phosphorylation sites (S202 and S226) in the linker and one in the C-terminus of the MH1 domain (S146) were mutated to alanine (Fig. 6C). Surprisingly, a construct expressing Mad in which these four sites were altered to alanine residues (Mad-4SA) was still phosphorylated by Nemo (Fig. 6D).

BMP receptor activation leads to phosphorylation of serines (SSVS) at the C-terminus of Mad (reviewed by ten Dijke and Hill, 2004). A Mad construct in which these sites were altered (Mad-AAVA; Fig. 6C) was also still phosphorylated by Nemo (Fig. 6D), ruling out these residues as possible Nemo target sites.

To map the domain in which the target residue was located, a truncated Mad protein was generated from which the MH1 domain was deleted (Mad-ΔMH1; Fig. 6C). This protein was no longer phosphorylated by Nemo (Fig. 6D), indicating that the target site was contained within the deleted fragment. Within the deleted MH1 fragment there are two putative Nemo target sites, S25 and S146. Since the S146 residue had been altered in the Mad-4SA construct that was still phosphorylated by Nemo, we focused on S25. Site-directed mutagenesis of S25A was performed and in vitro kinase assays from transfected cells revealed that Nemo was unable to phosphorylate MadS25A (Fig. 6D). Thus, we determined that Nemo can phosphorylate the single serine 25 residue in the MH1 domain of Mad. This residue has not previously been shown to be targeted by any MAPK proteins and has not previously been implicated in regulation of Mad function. The serine found in Mad at position 25 is conserved in the mammalian ortholog Smad1, but not in the related Smads 2 and 3.

Nemo blocks Tkv-dependent nuclear accumulation of Mad

Activation of BMP signaling leads to nuclear accumulation of receptor-phosphorylated Smads (reviewed by ten Dijke and Hill, 2004). In vertebrate cell culture experiments, Erk MAPK can inhibit this nuclear localization through its phosphorylation of Smads in the linker domain (reviewed by Massague, 2003). Since we have shown that Nemo can also phosphorylate Mad, we examined whether this affected the nuclear localization of Mad in transfected cells. Transfection of COS-7 cells with T7-Mad resulted in a uniform subcellular distribution of Mad (Fig. 7A). Quantitation showed that Mad expression is nuclear in 11.9% of transfected COS-7 cells (n=388), and cytoplasmic in the remaining cells. Co-transfection of an activated Tkv receptor (tkv^{QD}) led to the dramatic nuclear accumulation of Mad (91.2% of cells; n=457; Fig. 7B). This nuclear localization was inhibited by co-transfection of wild-type Nemo with Mad and Tkv (Fig. 7C). Quantitation showed that Mad is nuclear in 40.1% (n=424) of transfected cells. This effect is kinase-dependent, as transfection with kinase-dead Nemo (K69M) was unable to inhibit nuclear accumulation of Mad (Fig. 7D), with 87.1% of cells (n=417) showing nuclear Mad.

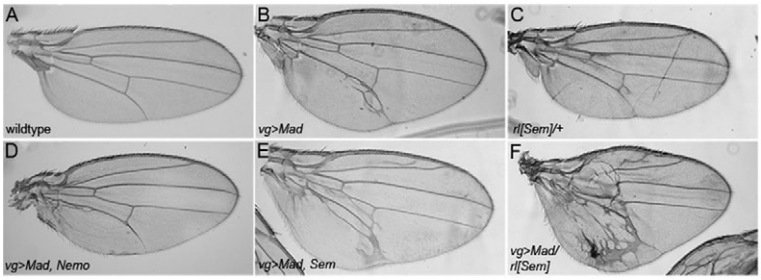

Fig. 5. The inhibition of Mad is specific to Nemo and not Erk MAPK. (**A**) A wild-type adult *Drosophila* wing. (**B**) The extra vein phenotype induced by *vg>Mad*. (**C**) A wing from a rl^{Sem}/+ hypermorphic fly. (**D**) Co-expression of *UAS-nmo* suppresses the *vg>Mad* phenotype. (**E**) Co-expression of *UAS-*rl^{Sem} (indicated as Sem) enhances the *vg>Mad* phenotype (**F**) Heterozygosity for the rl^{Sem} mutant enhances the *vg>Mad* phenotype.

Nemo phosphorylation of Mad promotes nuclear export

Examination of the subcellular localization of the MadS25A protein in COS-7 and HeLa cells revealed a primarily nuclear localization as compared with wild-type Mad (compare Fig. 7E and Fig. 8A with Fig. 7A). Significantly, the nuclear localization was found to be constitutive and unaffected by either expression of activated receptor or the presence of Nemo (data not shown). This suggests that the phosphorylation of Mad by Nemo at S25 regulates its nuclear accumulation, and this regulation is disrupted when the residue is rendered immune to Nemo phosphorylation (MadS25A). Consistent with the prediction that the phosphorylation status of S25 influences the localization of Mad, we found that MadS25D was localized primarily in the cytoplasm (Fig. 8B), even in the presence of activated receptor (data not shown).

Such observations suggest that Nemo is either involved in cytoplasmic sequestration of Mad or that phosphorylation by Nemo increases its rate of nuclear export. In both scenarios, the result would be removal of Mad from the nucleus and reduced target gene expression. To test which of these roles Nemo is carrying out, we examined the effect of leptomycin B (LMB) on Mad localization. LMB acts to inhibit Crm1 (Emb – Flybase) -dependent nuclear export, a process involved in the nucleocytoplasmic shuttling of BMP Smads, but not TGF-β Smads (Inman et al., 2002; Xiao et al., 2001). If Nemo is required for cytoplasmic tethering of Mad, then LMB treatment should not affect the cytoplasmic localization of Mad after co-transfection with Nemo. If, however, Nemo participates in stimulating nuclear export, then treatment with LMB should result in Mad accumulation in the nucleus, even in the presence of Nemo. We found that the nuclear retention of Mad

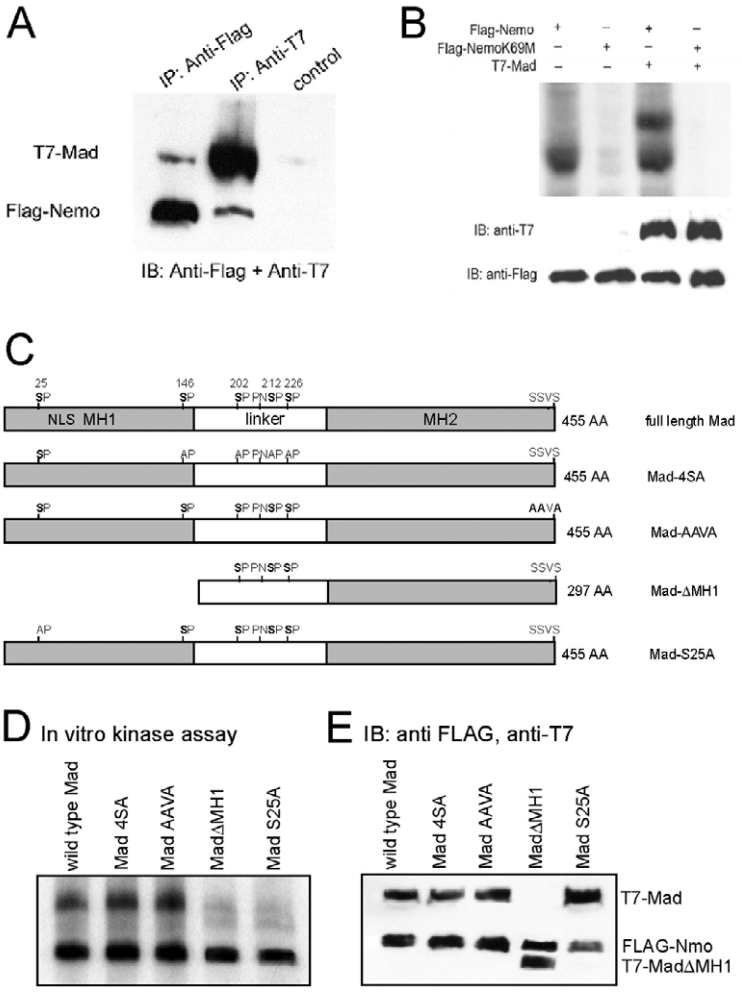

Fig. 6. *Drosophila* Nemo binds to and phosphorylates serine 25 in the MH1 domain of Mad. (**A**) pXJ-Flag-nemo and pCMV-T7-mad were co-transfected into HEK293 cells. Cell lysates were immunoprecipitated with anti-Flag, anti-T7 or IgG (control). Immunoblotting was performed with anti-Flag and anti-T7 antibodies. (**B**) Nemo phosphorylates Mad and autophosphorylates. HEK293 cells were transfected with expression vectors as indicated. Immunoprecipitated complexes with indicated antibodies were subjected to in vitro kinase assays and analyzed by autoradiography. The immunoprecipitates were also immunoblotted with the indicated antibodies to confirm loading. (**C**) Schematic of the full-length Mad protein showing the MH1, MH2 and linker domains, as well as the site of the nuclear localization sequence (NLS). Potential Nemo phosphorylation sites are each indicated directly above the protein structure as a numbered S residue, followed by proline (P). The constructs shown beneath were generated to identify residues that are phosphorylated by Nemo. (**D**) In vitro kinase assays performed with wild-type Mad, Mad 4SA, Mad AAVA, Mad-ΔMH1 and MadS25A demonstrate that Nemo specifically targets serine 25, and that Nemo autophosphorylates. (**E**) Immunoblot of cell extracts used in kinase assays showing relative expression levels of these proteins.

increased upon treatment with LMB (Fig. 8E,F), supporting the second scenario, i.e. that Nemo acts to promote nuclear export of Mad, thus reducing the effectiveness of Mad signaling.

In vivo consequences of the MadS25A mutation

To examine the potential role of the S25 residue in regulating Mad function, transgenic fly strains expressing a UAS-MadS25A transgene were generated. Expression of MadS25A was induced with numerous Gal4 drivers known to induce phenotypes upon expression of wild-type Mad. Since Mad proteins have to shuttle between the nucleus and cytoplasm to maintain their active state (Xiao et al., 2003; Xiao et al., 2001), our prediction would be that a nuclear-trapped Mad would signal weakly, at most. Consistent with this prediction, we found that in vivo expression of MadS25A with *engrailed-Gal4* (*en-Gal4*) resulted in very mild phenotypic consequences (Fig. 7G), as compared with the severe defects caused by expression of wild-type Mad (Fig. 7F). Among 20 independently generated transgenic lines, this S25A line displayed the strongest phenotypic consequences. In situ hybridizations performed with several independently isolated lines confirmed that the UAS transgenes were expressed (data not shown).

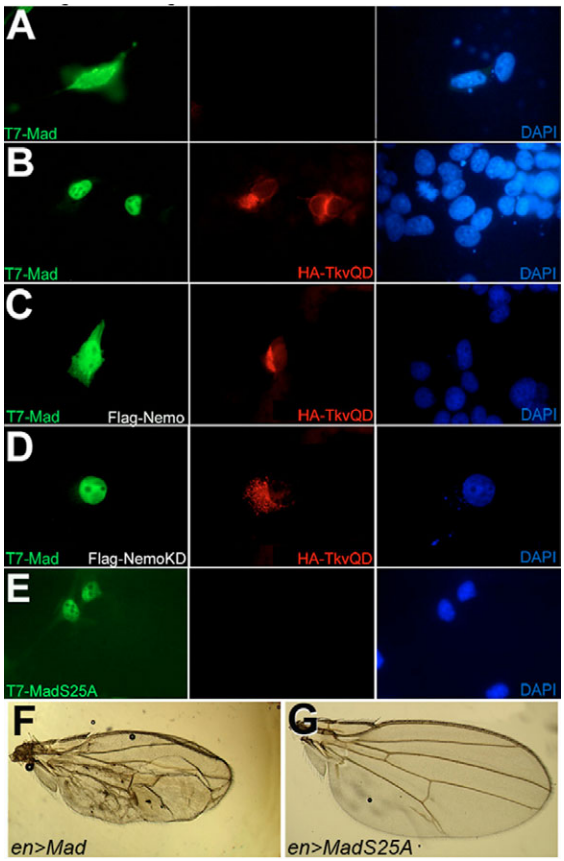

Fig. 7. *Drosophila* Nemo-mediated phosphorylation inhibits the nuclear accumulation of Mad and MadS25A shows receptor-independent nuclear localization. COS-7 cells were transfected with (**A**) T7-Mad; (**B**) T7-Mad and HA-Tkv^{QD} (constitutively active form); (**C**) T7-Mad, HA-Tkv^{QD} and Flag-Nemo; (**D**) T7-Mad, HA-Tkv^{QD} and Flag-NemoK69M (kinase-dead); (**E**) T7-MadS25A. Immunostaining was preformed using anti-T7 and anti-HA antibodies to indicate the localization of T7-Mad (left-hand column) and expression of HA-Tkv^{QD} (center column). DAPI staining was also performed prior to mounting (right-hand column). Expression of Nemo (C) can inhibit the Mad nuclear accumulation that occurs upon Tkv signaling (B). Expression of kinase-dead Nemo does not affect Mad localization (D). (E) Mutation of the Nemo target site renders MadS25A constitutively nuclear even in the absence of receptor activation. (**F**,**G**) In vivo consequences of *en-Gal4* expressing UAS-MadS25A (G) are very mild compared with wild-type UAS-Mad (F).

DISCUSSION

Nemo antagonizes BMP signaling by inhibition of Mad

In this study, we demonstrate a novel regulatory role for the *Drosophila* Nlk family member Nemo in a TGF-β-superfamily signal transduction pathway. We provide evidence that Nemo is an antagonist of BMP signaling in *Drosophila* by examining its role in wing development through genetic analysis and monitoring of BMP-dependent gene expression. The genetic interaction studies show that phenotypes caused by activation of the BMP pathway can be suppressed by ectopic *nmo* and enhanced by loss of *nmo*. Our data suggest that Nemo participates in the BMP pathway by modulating Mad activity. This is seen in the inhibition by Nemo of Mad-dependent gene expression and in the elevated expression of Mad target genes observed in *nmo* mutant clones. Nemo can bind to and phosphorylate Mad and this phosphorylation has direct consequences on the nuclear localization of Mad in cell culture. We mapped the single Nemo target residue to serine 25 within the MH1 domain of Mad, a site distinct from those previously implicated in the regulation of Mad activity and nuclear localization.

Regulation of Mad nuclear localization by phosphorylation

The vertebrate Mad ortholog Smad1 normally shuttles between the cytoplasm and nucleus in the absence of signal, but upon receptor activation becomes phosphorylated at its C-terminus, binds the Co-Smad and accumulates primarily in the nucleus (Xiao et al., 2001). Such nucleocytoplasmic shuttling is observed with R-Smads participating in both BMP and TGF-β signaling (reviewed by ten Dijke and Hill, 2004). The shuttling provides a tightly regulated mechanism for monitoring the activation status of the receptors (Inman et al., 2002). Receptor-phosphorylated Smads are dephosphorylated in the nucleus, most likely causing them to detach from Co-Smads and DNA and allowing them to shuttle back to the cytoplasm (Chen et al., 2006; Duan et al., 2006; Knockaert et al., 2006). Their nuclear retention is aided by the formation of the R-Smad–Co-Smad complex and DNA binding. Thus, receptor activation leads to elevated nuclear retention. The actual rates of nuclear import are not altered by receptor-mediated phosphorylation (Schmierer and Hill, 2005).

From our findings we conclude that under normal conditions, endogenous Nemo acts to modulate the level of active Mad that is retained in the nucleus. Since Nemo is expressed ubiquitously at low levels and is enriched in cells with elevated levels of pMad, it fulfils the requirements for such a molecule involved in fine-tuning the BMP response. The phosphorylation by Nemo might control a delicate balance between promoting cytoplasmic localization of Mad, while allowing certain levels of Mad signaling to proceed in a receptor-dependent manner.

Differential control of Mad by Nemo and Erk MAPKs

We show that Nemo can inhibit BMP signaling by antagonizing the nuclear localization of Mad in a kinase-dependent manner. Such a mechanism has been attributed previously to crosstalk between Erk

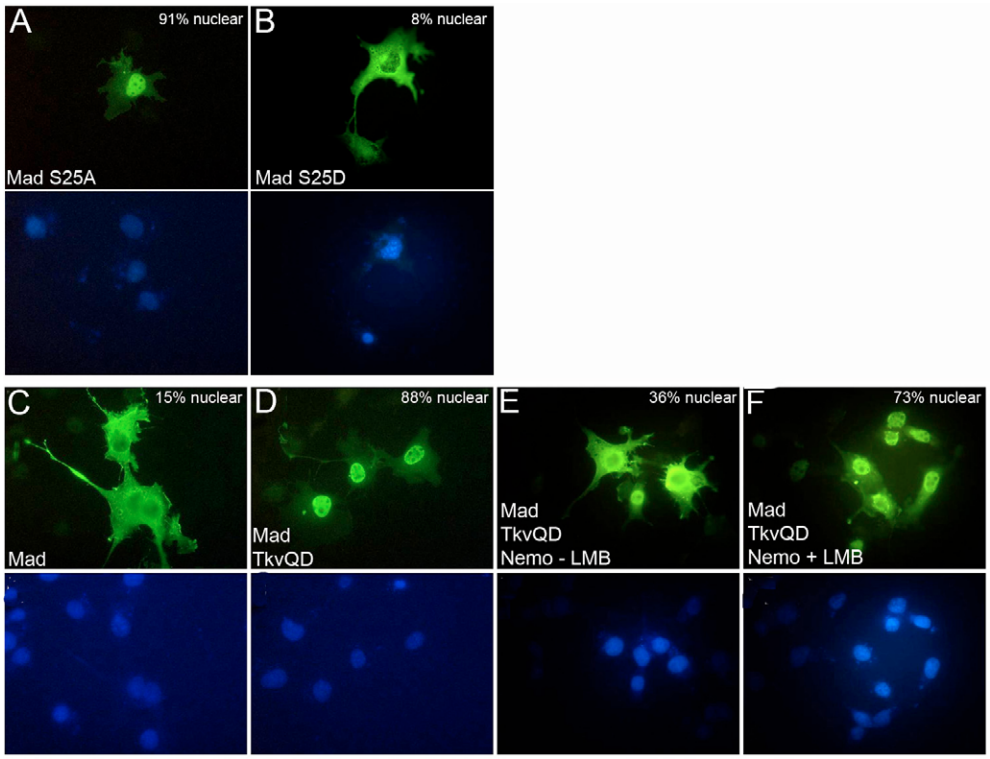

Fig. 8. *Drosophila* Nemo phosphorylation promotes the nuclear export of Mad. COS-7 cells were transfected with the constructs indicated and stained for the localization of Mad (green, upper panel of each pair) and with DAPI to indicate nuclei (blue, lower panel of each pair). MadS25A is primarily nuclear (**A**), whereas MadS25D is heavily enriched in the cytoplasm (**B**). Percentages indicate the number of cells displaying a primarily nuclear localization. (**C**,**D**) The localization of Mad is influenced by Tkv receptor activation. (**E**,**F**) Co-transfection of Nemo inhibits the Tkv-induced nuclear accumulation in the absence of leptomycin B (LMB) (E), but does not block nuclear retention in the presence of LMB (F).

MAPK signaling and TGF-β/BMP signaling (reviewed by Massague, 2003). Our research presents Nemo as the first MAPK-like protein to attenuate *Drosophila* BMP pathway activity through phosphorylation of Mad. We have also found that murine Nlk can bind to Mad (data not shown), raising the intriguing possibility that this mechanism is conserved across species.

MAPK can repress TGF-β-superfamily signaling by targeting several Smads (Aubin et al., 2004; Grimm and Gurdon, 2002; Kretzschmar et al., 1997; Kretzschmar et al., 1999; Pera et al., 2003). The BMP-specific Smad1 is a target of cross-regulation by EGF signaling through the Erk MAPK pathway. Erk phosphorylates Smad1 in the linker domain and inhibits both the nuclear accumulation and transcriptional activity of Smad1 in cell culture and, in consequence, the in vivo function of Smad1 in neural induction and tissue homeostasis (Aubin et al., 2004; Kretzschmar et al., 1997; Pera et al., 2003). Ras-stimulated Erk also phosphorylates two R-Smads involved in TGF-β/Activin signaling and prevents their nuclear accumulation (Kretzschmar et al., 1999). The phosphorylation sites within these Smads differ, thus providing a mechanism for preferentially selective inhibition of one subtype (reviewed by Massague, 2003). Thus, the distinct Nemo phosphorylation site in the MH1 domain represents an additional level of regulation of these proteins.

Interestingly, in our studies, we have found that the *Drosophila* Erk MAPK does not inhibit Mad during wing development. In fact, Erk and Mad appear to synergize in the wing blade, as would be predicted given that both Egfr and BMP signaling are required for vein specification.

Targeting of the Mad MH1 domain by Nemo kinase

The phosphorylation of serine 25 in the MH1 domain of Mad represents a novel site of regulation of Smads. This protein domain is involved in nuclear localization, DNA binding and association with transcriptional regulators (Kretzschmar and Massagué, 1998). Based on known protein structures of Smads, one can predict that the Mad MH1 domain is composed of several elements. The most N-terminal sequence predicts a flexible region, then a short alpha-helix followed by a linker region and a longer, second alpha-helix (Chai et al., 2003). The second alpha-helix contains the predicted nuclear localization sequence (NLS) (Xiao et al., 2001). Serine 25 is located just N-terminal to the first alpha-helix. The added negative charge following phosphorylation by Nemo could modify the interaction between the two alpha-helical regions by potentially neutralizing the positively charged NLS and thereby influencing nuclear localization of Mad. Such a model is also supported by our finding that mutation of serine to alanine renders Mad constitutively nuclear. Interestingly, Kretzschmar et al. (Kretzschmar et al., 1997) observed a similar constitutively nuclear localization when they mutated the Erk phosphorylation sites in Smad1. This suggests that both Nemo and Erk MAPK are involved in the inhibition of BMP signaling and that their distinct sites of action function to block the nuclear accumulation of Smads. Thus, the cellular factors that induce either Nlk or Erk activity can oppose the functions of BMP signaling.

In vivo inhibition of BMP signaling by Nemo during wing patterning and growth

In addition to the biochemical and cell culture evidence that Nemo targets the MH1 domain of Mad to promote its nuclear export, we present in vivo evidence which clearly demonstrates that the expression of Nemo or absence of *nmo* has a measurable effect on the readout of the BMP pathway in terms of Mad target gene expression, wing size, wing vein spacing and vein patterning. Specifically, elevated Nemo can attenuate the expression of vg^{Q} and *salm*, whereas *nmo* somatic clones and mutant discs show elevated or expanded target gene expression. Genetic interaction studies confirm such an antagonistic role, as elevated Nemo can suppress the mutant phenotypes induced by elevated BMP signaling, and reductions in

nmo enhanced the penetrance of activated BMP phenotypes. Thus, the phenotypic analyses support and extend the biochemical model of the inhibition of Mad and BMP signaling by Nemo.

Modulation of Nemo does not affect the levels of pMad found at the peaks of the BMP response gradients, suggesting that the effect of Nemo is at the level of the nuclear function of Mad. Our LMB studies demonstrate that Nemo can affect the nuclear localization of Mad. Thus, we propose that Nemo promotes the nuclear export of Mad and that this results in a fine-tuning of the levels of target genes in regions where *nmo* is expressed.

We propose that one role for *nmo* is in refining the level of BMP signaling regulating proliferation. This early role for BMP signaling also relies on Mad and is therefore a candidate for Nemo-mediated inhibition. The effect on proliferation may affect the spacing, but not levels, of the pMad gradient. We consistently observe that the genotypes in which wing width is affected do have a mild effect on the spacing of pMad stripes, and we suggest this might be due to actual changes in cell number in the disc. Additionally, *nmo* mutations manifest in alterations in wing size, wing shape and cell density.

nmo mutations also affect the later larval and pupal patterning and differentiation functions of BMP, and these can be correlated to changes in target gene expression and with vein patterning abnormalities. Thus, it appears that Nemo can modulate levels of BMP signaling at several developmental stages in wing growth and patterning.

Nlks integrate multiple signaling pathways during development

We have previously demonstrated that Nemo can antagonize *Drosophila* Wg signaling during wing development (Zeng and Verheyen, 2004). In this study we demonstrate that Nemo also acts to attenuate BMP signaling by targeting the activity of Mad. In both of these signaling pathways the net outcome is the inhibition by Nemo of pathway-dependent target gene expression. These results demonstrate that Nemo – and by extension the Nemo-like kinases – play important roles in refining signaling pathways during development.

An intriguing but still incomplete picture is emerging regarding the regulation of both Nlk expression and activity and it represents a potential point of crosstalk between signaling pathways. We have shown that *nmo* is transcriptionally regulated by Wg signaling (Zeng and Verheyen, 2004). Others have found that the kinase activity of Nlk is stimulated by Tak1 after Wnt induction (Ishitani et al., 2003a; Smit et al., 2004; Kanei-Ishii et al., 2004) and that Tak1 can be activated by BMP signaling (Yamaguchi et al., 1995). Activated Nlk can inhibit Tcf/Lef proteins and modulate Wnt-dependent gene expression (Ishitani et al., 2003b; Ishitani et al., 1999; Zeng and Verheyen, 2004). In this study, we found that *Drosophila* Nlk is playing an important role in modulating BMP signaling and Mad-dependent gene expression, revealing an additional point of cross-regulation and refinement between signaling molecules.

We are grateful to many researchers for providing fly strains and reagents: L. Raftery, H. Nakagoshi, T. Imamura, D. Wotton, E. Bier, K. Wharton, K. Basler, E. Hafen, S. Cohen, T. Tabata, G. Campbell, P. ten Dijke, R. Bario, M. Go, M. Leroux and the Bloomington *Drosophila* Stock Center. We thank D. Bessette for generating the kinase-dead Nemo construct; M. Trapp and L. Quarmby for microscopy assistance; M. Leroux for the use of his tissue culture facility; and L. Raftery, K. Wharton, P. Haghighi, N. Harden, H. Clevers and members of the Verheyen laboratory for helpful discussions and comments. Y.A.Z. was supported by a MacMillan Bloedel Graduate Scholarship. This work was supported by an operating grant from the Canadian Institutes of Health Research (CIHR).

References

Attisano, L. and Wrana, J. L. (2002). Signal transduction by the TGF-beta superfamily. *Science* **296**, 1646-1647.
Aubin, J., Davy, A. and Soriano, P. (2004). In vivo convergence of BMP and MAPK signaling pathways: impact of differential Smad1 phosphorylation on development and homeostasis. *Genes Dev.* **18**, 1482-1494.
Bangi, E. and Wharton, K. (2006). Dpp and Gbb exhibit different effective ranges in the establishment of the BMP activity gradient critical for Drosophila wing patterning. *Dev. Biol.* **295**, 178-193.
Barrio, R. and de Celis, J. F. (2004). Regulation of spalt expression in the Drosophila wing blade in response to the Decapentaplegic signaling pathway. *Proc. Natl. Acad. Sci. USA* **101**, 6021-6026.
Behrens, J. (2000). Cross-regulation of the Wnt signalling pathway: a role of MAP kinases. *J. Cell Sci.* **113**, 911-919.
Bier, E. (2000). Drawing lines in the Drosophila wing: initiation of wing vein development. *Curr. Opin. Genet. Dev.* **10**, 393-398.
Brand, A. and Perrimon, N. (1993). Targetted gene expression as a means of altering cell fates and generating dominant phenotypes. *Development* **118**, 401-415.
Brott, B. K., Pinsky, B. A. and Reikson, R. L. (1998). Nlk is a murine protein kinase related to Erk/MAP kinases and localized in the nucleus. *Proc. Natl. Acad. Sci. USA* **95**, 963-968.
Brummel, T. J., Twombly, V., Marques, G., Wrana, J. L., Newfeld, S. J., Attisano, L., Massague, J., O'Connor, M. B. and Gelbart, W. M. (1994). Characterization and relationship of Dpp receptors encoded by the saxophone and thick veins genes in Drosophila. *Cell* **78**, 251-261.
Brunner, D., Oellers, N., Szabad, J., Biggs, W., Zipursky, S. and Hafen, E. (1994). A gain-of-function mutation in Drosophila MAP kinase activates multiple receptor tyrosine kinase signaling pathways. *Cell* **76**, 875-888.
Burke, R. and Basler, K. (1996). Dpp receptors are autonomously required for cell proliferation in the entire developing Drosophila wing. *Development* **122**, 2261-2269.
Chai, J., Wu, J. W., Yan, N., Massague, J., Pavletich, N. P. and Shi, Y. (2003). Features of a Smad3 MH1-DNA complex. Roles of water and zinc in DNA binding. *J. Biol. Chem.* **278**, 20327-20331.
Chen, H. B., Shen, J., Ip, Y. T. and Xu, L. (2006). Identification of phosphatases for Smad in the BMP/DPP pathway. *Genes Dev.* **20**, 648-653.
Choi, K.-W. and Benzer, S. (1994). Rotation of photoreceptor clusters in the developing *Drosophila* eye requires the *nemo* gene. *Cell* **78**, 125-136.
Conley, C., Silburn, R., Singer, M., Ralston, A., Rohwer-Nutter, D., Olson, D., Gelbart, W. and Blair, S. (2000). Crossveinless 2 contains cysteine-rich domains and is required for high levels of BMP-like activity during the formation of the cross veins in Drosophila. *Development* **127**, 3947-3959.
Cook, O., Biehs, B. and Bier, E. (2004). brinker and optomotor-blind act coordinately to initiate development of the L5 wing vein primordium in Drosophila. *Development* **131**, 2113-2124.
de Celis, J. F. (1997). Expression and function of decapentaplegic and thick veins during the differentiation of the veins in the Drosophila wing. *Development* **124**, 1007-1018.
Duan, X., Liang, Y. Y., Feng, X. H. and Lin, X. (2006). Protein serine/threonine phosphatase PPM1A dephosphorylates Smad1 in the bone morphogenetic protein signaling pathway. *J. Biol. Chem.* **281**, 36526-36532.
Golan, T., Yaniv, A., Bafico, A., Liu, G. and Gazit, A. (2004). The human Frizzled 6 (HFz6) acts as a negative regulator of the canonical Wnt. beta-catenin signaling cascade. *J. Biol. Chem.* **279**, 14879-14888.
Grimm, O. H. and Gurdon, J. B. (2002). Nuclear exclusion of Smad2 is a mechanism leading to loss of competence. *Nat. Cell Biol.* **4**, 519-522.
Grimm, S. and Pflugfelder, G. O. (1996). Control of the gene optomotor-blind in Drosophila wing development by *decapentaplegic* and *wingless*. *Science* **271**, 1601-1604.
Haerry, T. E., Khalsa, O., O'Connor, M. B. and Wharton, K. A. (1998). Synergistic signaling by two BMP ligands through the SAX and TKV receptors controls wing growth and patterning in Drosophila. *Development* **125**, 3977-3987.
Hudson, J. B., Podos, S. D., Keith, K., Simpson, S. L. and Ferguson, E. L. (1998). The Drosophila Medea gene is required downstream of dpp and encodes a functional homolog of human Smad4. *Development* **125**, 1407-1420.
Hyodo-Miura, J., Urushiyama, S., Nagai, S., Nishita, M., Ueno, N. and Shibuya, H. (2002). Involvement of NLK and Sox11 in neural induction in Xenopus development. *Genes Cells* **7**, 487-496.
Inman, G. J., Nicolas, F. J. and Hill, C. S. (2002). Nucleocytoplasmic shuttling of Smads 2, 3, and 4 permits sensing of TGF-beta receptor activity. *Mol. Cell* **10**, 283-294.
Inoue, H., Imamura, T., Ishidou, Y., Takase, M., Udagawa, Y., Oka, Y., Tsuneizumi, K., Tabata, T., Miyazono, K. and Kawabata, M. (1998). Interplay of signal mediators of decapentaplegic (Dpp): molecular characterization of mothers against dpp, Medea, and daughters against dpp. *Mol. Biol. Cell* 9, 2145-2156.
Ishitani, T., Ninomiya-Tsuji, J., Nagai, S., Nishita, M., Meneghini, M., Barker,

N., Waterman, M., Bowerman, B., Clevers, H., Shibuya, H. et al. (1999). The TAK1-NLK-MAPK-related pathway antagonizes signalling between beta-catenin and transcription factor TCF. *Nature* **399**, 798-802.
Ishitani, T., Kishida, S., Hyodo-Miura, J., Ueno, N., Yasuda, J., Waterman, M., Shibuya, H., Moon, R. T., Ninomiya-Tsuji, J. and Matsumoto, K. (2003a). The TAK1-NLK mitogen-activated protein kinase cascade functions in the Wnt-5a/Ca(2+) pathway to antagonize Wnt/beta-catenin signaling. *Mol. Cell. Biol.* **23**, 131-139.
Ishitani, T., Ninomiya-Tsuji, J. and Matsumoto, K. (2003b). Regulation of lymphoid enhancer factor 1/T-cell factor by mitogen-activated protein kinase-related Nemo-like kinase-dependent phosphorylation in Wnt/beta-catenin signaling. *Mol. Cell. Biol.* **23**, 1379-1389.
Ito, K., Awano, W., Suzuki, K., Hiromi, Y. and Yamamoto, D. (1997). The Drosophila mushroom body is a quadruple structure of clonal units each of which contains a virtually identical set of neurones and glial cells. *Development* **124**, 761-771.
Kanei-Ishii, C., Ninomiya-Tsuji, J., Tanikawa, J., Nomura, T., Ishitani, T., Kishida, S., Kokura, K., Kurahashi, T., Ichikawa-Iwata, E., Kim, Y. et al. (2004). Wnt-1 signal induces phosphorylation and degradation of c-Myb protein via TAK1, HIPK2, and NLK. *Genes Dev.* **18**, 816-829.
Khalsa, O., Yoon, J. W., Torres-Schumann, S. and Wharton, K. A. (1998). TGF-beta/BMP superfamily members, Gbb-60A and Dpp, cooperate to provide pattern information and establish cell identity in the Drosophila wing. *Development* **125**, 2723-2734.
Kim, J., Johnson, K., Chen, H. J., Carroll, S. and Laughon, A. (1997). Drosophila Mad binds to DNA and directly mediates activation of vestigial by Decapentaplegic. *Nature* **388**, 304-308.
Knockaert, M., Sapkota, G., Alarcon, C., Massague, J. and Brivanlou, A. H. (2006). Unique players in the BMP pathway: small C-terminal domain phosphatases dephosphorylate Smad1 to attenuate BMP signaling. *Proc. Natl. Acad. Sci. USA* **103**, 11940-11945.
Kretzschmar, M. and Massague, J. (1998). SMADs: mediators and regulators of TGF-beta signaling. *Curr. Opin. Genet. Dev.* **8**, 103-111.
Kretzschmar, M., Doody, J. and Massague, J. (1997). Opposing BMP and EGF signalling pathways converge on the TGF-beta family mediator Smad1. *Nature* **389**, 618-622.
Kretzschmar, M., Doody, J., Timokhina, I. and Massague, J. (1999). A mechanism of repression of TGFbeta/ Smad signaling by oncogenic Ras. *Genes Dev.* **13**, 804-816.
Lecuit, T. and Cohen, S. M. (1998). Dpp receptor levels contribute to shaping the Dpp morphogen gradient in the Drosophila wing imaginal disc. *Development* **125**, 4901-4907.
Lecuit, T., Brook, W. J., Ng, M., Calleja, M., Sun, H. and Cohen, S. M. (1996). Two distinct mechanisms for long-range patterning by Decapentaplegic in the Drosophila wing. *Nature* **381**, 387-393.
Martin-Castellanos, C. and Edgar, B. A. (2002). A characterization of the effects of Dpp signaling on cell growth and proliferation in the Drosophila wing. *Development* **129**, 1003-1013.
Martinez Arias, A., Brown, A. M. and Brennan, K. (1999). Wnt signalling: pathway or network? *Curr. Opin. Genet. Dev.* **9**, 447-454.
Marquez, R. M., Singer, M. A., Takaesu, N. T., Waldrip, W. R., Kraytsberg, Y. and Newfeld, S. J. (2001). Transgenic analysis of the Smad family of TGF-beta signal transducers in Drosophila melanogaster suggests new roles and new interactions between family members. *Genetics* **157**, 1639-1648.
Massague, J. (2003). Integration of Smad and MAPK pathways: a link and a linker revisited. *Genes Dev.* **17**, 2993-2997.
Meneghini, M. D., Ishitani, T., Carter, J. C., Hisamoto, N., Ninomiya-Tsuji, J., Thorpe, C. J., Hamill, D. R., Matsumoto, K. and Bowerman, B. (1999). MAP kinase and Wnt pathways converge to downregulate an HMG-domain repressor in Caenorhabditis elegans. *Nature* **399**, 793-797.
Mirkovic, I., Charish, K., Gorski, S. M., McKnight, K. and Verheyen, E. M. (2002). Drosophila nemo is an essential gene involved in the regulation of programmed cell death. *Mech. Dev.* **119**, 9-20.
Moustakas, A., Souchelnytskyi, S. and Heldin, C. H. (2001). Smad regulation in TGF-beta signal transduction. *J. Cell Sci.* **114**, 4359-4369.
Nellen, D., Burke, R., Struhl, G. and Basler, K. (1996). Direct and long-range action of a DPP morphogen gradient. *Cell* **85**, 357-368.
Ohkawara, B., Shirakabe, K., Hyodo-Miura, J., Matsuo, R., Ueno, N., Matsumoto, K. and Shibuya, H. (2004). Role of the TAK1-NLK-STAT3 pathway in TGF-beta-mediated mesoderm induction. *Genes Dev.* **18**, 381-386.
Padgett, R. W., St. Johnston, R. D. and Gelbart, W. M. (1987). A transcript from a Drosophila pattern gene predicts a protein homologous to the transforming growth factor-beta family. *Nature* **325**, 81-84.
Pera, E. M., Ikeda, A., Eivers, E. and De Robertis, E. M. (2003). Integration of IGF, FGF, and anti-BMP signals via Smad1 phosphorylation in neural induction. *Genes Dev.* **17**, 3023-3028.
Persson, U., Izumi, H., Souchelnytskyi, S., Itoh, S., Grimsby, S., Engstrom, U., Heldin, C. H., Funa, K. and ten Dijke, P. (1998). The L45 loop in type I receptors for TGF-beta family members is a critical determinant in specifying Smad isoform activation. *FEBS Lett.* **434**, 83-87.
Raftery, L. A. and Sutherland, D. J. (1999). TGF-beta family signal transduction in Drosophila development: from Mad to Smads. *Dev. Biol.* **210**, 251-268.
Rintelen, F., Hafen, E. and Nairz, K. (2003). The Drosophila dual-specificity ERK phosphatase DMKP3 cooperates with the ERK tyrosine phosphatase PTP-ER. *Development* **130**, 3479-3490.
Rocheleau, C. E., Yasuda, J., Shin, T. H., Lin, R., Sawa, H., Okano, H., Priess, J. R., Davis, R. J. and Mello, C. C. (1999). WRM-1 activates the LIT-1 protein kinase to transduce anterior/posterior polarity signals in C. elegans. *Cell* **97**, 717-726.
Rogulja, D. and Irvine, K. D. (2005). Regulation of cell proliferation by a morphogen gradient. *Cell* **123**, 449-461.
Schmierer, B. and Hill, C. S. (2005). Kinetic analysis of Smad nucleocytoplasmic shuttling reveals a mechanism for transforming growth factor beta-dependent nuclear accumulation of Smads. *Mol. Cell. Biol.* **25**, 9845-9858.
Segal, D. and Gelbart, W. M. (1985). Shortvein, a new component of the decapentaplegic gene complex in Drosophila melanogaster. *Genetics* **109**, 119-143.
Shi, Y. and Massague, J. (2003). Mechanisms of TGF-beta signaling from cell membrane to the nucleus. *Cell* **113**, 685-700.
Shin, T., Yasuda, J., Rocheleau, C., Lin, R., Soto, M., Bei, X., Davis, R. and Mello, C. (1999). MOM-4, a MAP kinase kinase kinase-related protein, activates WRM-1/LIT-1 kinase to transduce anterior/posterior polarity signals in *C. elegans*. *Mol. Cell* **4**, 275-280.
Smit, L., Baas, A., Kuipers, J., Korswagen, H., van de Wetering, M. and Clevers, H. (2004). Wnt activates the Tak1/Nemo-like kinase pathway. *J. Biol. Chem.* **279**, 17232-17240.
Spencer, F. A., Hoffmann, F. M. and Gelbart, W. M. (1982). Decapentaplegic: a gene complex affecting morphogenesis in Drosophila melanogaster. *Cell* **28**, 451-461.
Sturtevant, M. A., Biehs, B., Marin, E. and Bier, E. (1997). The spalt gene links the A/P compartment boundary to a linear adult structure in the Drosophila wing. *Development* **124**, 21-32.
Tanimoto, H., Itoh, S., ten Dijke, P. and Tabata, T. (2000). Hedgehog creates a gradient of DPP activity in Drosophila wing imaginal discs. *Mol. Cell* **5**, 59-71.
ten Dijke, P. and Hill, C. S. (2004). New insights into TGF-beta-Smad signalling. *Trends Biochem. Sci.* **29**, 265-273.
Thorpe, C. J. and Moon, R. T. (2004). nemo-like kinase is an essential co-activator of Wnt signaling during early zebrafish development. *Development* **131**, 2899-2909.
Tsuneizumi, K., Nakayama, T., Kamoshida, Y., Kornberg, T. B., Christian, J. L. and Tabata, T. (1997). Daughters against dpp modulates dpp organizing activity in Drosophila wing development. *Nature* **389**, 627-631.
Verheyen, E. M., Mirkovic, I., MacLean, S. J., Langmann, C., Andrews, B. C. and MacKinnon, C. (2001). The tissue polarity gene *nemo* carries out multiple roles in patterning during Drosophila development. *Mech. Dev.* **101**, 119-132.
von Bubnoff, A. and Cho, K. W. (2001). Intracellular BMP signaling regulation in vertebrates: pathway or network? *Dev. Biol.* **239**, 1-14.
Wharton, K. A., Thomsen, G. H. and Gelbart, W. M. (1991). Drosophila 60A gene, another transforming growth factor beta family member, is closely related to human bone morphogenetic proteins. *Proc. Natl. Acad. Sci. USA* **88**, 9214-9218.
Xiao, Z., Watson, N., Rodriguez, C. and Lodish, H. F. (2001). Nucleocytoplasmic shuttling of Smad1 conferred by its nuclear localization and nuclear export signals. *J. Biol. Chem.* **276**, 39404-39410.
Xiao, Z., Brownawell, A. M., Macara, I. G. and Lodish, H. F. (2003). A novel nuclear export signal in Smad1 is essential for its signaling activity. *J. Biol. Chem.* **278**, 34245-34252.
Xu, T. and Rubin, G. M. (1993). Analysis of genetic mosaics in developing and adult Drosophila tissues. *Development* **117**, 1223-1237.
Yamaguchi, K., Shirakabe, K., Shibuya, H., Irie, K., Oishi, I., Ueno, N., Taniguchi, T., Nishida, E. and Matsumoto, K. (1995). Identification of a member of the MAPKKK family as a potential mediator of TGF-beta signal transduction. *Science* **270**, 2008-2011.
Yamada, M., Ohkawara, B., Ichimura, N., Hyodo-Miura, J., Urushiyama, S., Shirakabe, K. and Shibuya, H. (2003). Negative regulation of Wnt signalling by HMG2L1, a novel NLK-binding protein. *Genes Cells* **8**, 677-684.
Yasuda, J., Yokoo, H., Yamada, T., Kitabayashi, I., Sekiya, T. and Ichikawa, H. (2004). Nemo-like kinase suppresses a wide range of transcription factors, including nuclear factor-kappaB. *Cancer Sci.* **95**, 52-57.
Yu, K., Sturtevant, M. A., Biehs, B., Francois, V., Padgett, R. W., Blackman, R. K. and Bier, E. (1996). The Drosophila decapentaplegic and short gastrulation genes function antagonistically during adult wing vein development. *Development* **122**, 4033-4044.
Yu, K., Srinivasan, S., Shimmi, O., Biehs, B., Rashka, K. E., Kimelman, D., O'Connor, M. B. and Bier, E. (2000). Processing of the Drosophila Sog protein creates a novel BMP inhibitory activity. *Development* **127**, 2143-2154.
Zecca, M., Basler, K. and Struhl, G. (1996). Direct and long-range action of a wingless morphogen gradient. *Cell* **87**, 833-844.
Zeng, Y. A. and Verheyen, E. M. (2004). Nemo is an inducible antagonist of Wingless signaling during Drosophila wing development. *Development* **131**, 2911-2920.